Kettunen, Markus; Jämsä-Jounela, Sirkka-Liisa

Data-Based, Fault-Tolerant Model Predictive Control of a Complex Industrial Dearomatization Process

Published in:
Industrial and Engineering Chemistry Research

DOI:
10.1021/ie102312g

Published: 01/01/2011

Document Version
Peer-reviewed accepted author manuscript, also known as Final accepted manuscript or Post-print

Please cite the original version:
Kettunen, M., & Jämsä-Jounela, S.-L. (2011). Data-Based, Fault-Tolerant Model Predictive Control of a Complex Industrial Dearomatization Process. *Industrial and Engineering Chemistry Research*, *50*(11), 6755-6768. https://doi.org/10.1021/ie102312g

Author's accepted manuscript, published in Industrial & Engineering Research 50 (2011) 6755-6768

Data-based, fault-tolerant model predictive control of a complex industrial dearomatization process

Markus Kettunen and Sirkka-Liisa Jämsä-Jounela

Aalto University School of Chemical Technology, Department of Biotechnology and Chemical Technology, Laboratory of Process Control and Automation, POB 16100, FI-00076 AALTO, Finland.

Abstract:

The main focus of this paper is on the development of an active data-based fault-tolerant model predictive controller (FTMPC) for an industrial dearomatization process. Three different fault-tolerant control (FTC) strategies are presented; these comprise data-based fault detection and diagnosis (FDD) methods and fault accommodation- and controller reconfiguration-based FTC methods. These three strategies are tested with the simulated industrial dearomatization process. According to the validation and performance testing, the FTMPC performs efficiently and detects and prevents the effects of the most common faults in the analyser, flow and temperature measurements as well as the controller actuators. The reliability of the model predictive controller (MPC) is increased and the profitability is enhanced due to the lower off-spec production.

1 Introduction

Tightened global competition, higher final product quality requirements and environmental and safety regulations have forced the oil refining industry to continuously enhance and optimise the efficiency and profitability of its process plants. Profitability can generally be enhanced through process optimisation, by cutting costs and by reducing the duration of planned and unplanned shutdowns. Optimisation can further be enhanced by focusing on preventing the off-spec production caused by process disturbances and faults. The effect of faults and process disturbances on the target process can be prevented by using FTC strategies, which are generally categorised into passive and active approaches as described by Venkatasubramanian et al. [1] and Zhang and Jiang[2], for example. According to Venkatasubramanian et al.[1], approximately 70% of industrial accidents are caused by human errors and over USD 20 billion are lost annually in the North American oil refining industry alone due to the improper handling of abnormal situations. There is a clear need, therefore, for automated FTC applications in the oil refining industry.

Passive FTC, such as robust MPC originally developed by Campo and Morari[3], aims at improving the robustness of the controller against faults and disturbances by modelling the effects of the faults and disturbances, and by taking them into account in the objective function of the MPC. A common approach for passive FTC is the min–max-based robust MPC, where the goal is to maximise the performance of the MPC by minimising the worst-case tracking error (the largest difference between the prediction and the actual measurement) of the predictive controller. This is accomplished by adding the estimation of the uncertainties (faults, disturbances) as an input to the predictive controller and taking it into account in the MPC objective function. Recent notable robust MPC strategies include the optimal min–max-based controller by Bemporad et al.[4]; the min–max-based controller for the discrete nonlinear systems by Lazar et al.[5]; and the recent nonlinear robust approach by Huang et al.[6].

Active FTC, on the other hand, attempts to reduce the fault effects by using active FTC elements and methods. These active elements include the FDD components for the detection, isolation and identification of faults, and the FTC components carrying out active fault accommodation or controller reconfiguration actions to reduce the effects of the faults. The fault isolation part of the FDD is particularly important in the complex safety-critical processes, since the detection of a fault in the wrong variable could have catastrophic consequences.

The potentially most effective active approaches within the last decade include the data- and fault-accommodation-based FTC strategy for the simulated FCC unit by Pranatyasto and Qin[7]; the supervisory model- and fault accommodation-based approach by Prakash et al.[8]; the nonlinear controller reconfiguration-based strategy by Mhaskar et al.[9]; the application-oriented data-based reconfigurable FTC by Koivisto et al.[10]; and the nonlinear model-based strategy by Deshpande et al.[11].

In order to meet the challenges related to reducing the effects of different fault types, the goals for this paper are to demonstrate the improvement in the control performance and profitability of a simulated industrial dearomatization process affected by sensor and actuator faults. The performance and profitability improvements are gained through the utilisation of active FTC strategies, which take into account faults in the analyser, flow, temperature and pressure measurements as well as in the actuators. The main contribution and novelty of this paper is the integrated FTMPC containing the three parallel-running active data-based FTC strategies that are also discussed by Kettunen[12].

To meet the established goals, Section 2 of this article first outlines the proposed integrated fault-tolerant MPC. Section 3 presents the target dearomatization process, the control objectives and variables; the faults in the target process are given; and finally, the testing environment is described. Section 4 presents the results of the FTMPC testing and the economic evaluation. Finally, Section 5 concludes the article by stating the importance of the active FTC for the optimal control of a complex industrial dearomatization process.

2 Data-based fault-tolerant model predictive control

In complex industrial processes, such as oil refining, faults in actuators, sensors and process components are common, although highly undesired phenomena that have a significant effect on the quality of the final products and production efficiency. A fault is also defined as an unpermitted deviation of at least one characteristic property or parameter of the system from the acceptable behaviour[13]. In essence, a fault is defined as a state that may lead to a malfunction or a failure. Some examples of typical faults for feedback controllers are a burned-out thermocouple, a broken transducer or a stuck valve[14]. For sensors such as a temperature or a flow measurement, the most typical fault types are a bias fault, a complete failure, a drifting fault and a precision degradation fault[15]. Therefore, increasing the robustness of individual control system components may not be sufficient to maintain a high level of control performance. A completely different approach, such as an active fault-tolerant MPC, is thus required to improve the MPC's reliability under effects of disturbances and faults in a control system's components.

2.1 General structure of the active integrated fault-tolerant MPC

An effective industrial fault-tolerant MPC integrates both fault accommodation and controller reconfiguration strategies in order to be able to successfully handle a wide range of faults; further, the main task of an active, integrated fault-tolerant MPC is to extract information from process data and to ensure optimal operation when faults also affect the control system components. The behaviour of the target process can be captured by applying statistical mathematical methods, such as partial least squares (PLS) to process history data. In general, PLS is recommended as the most suitable candidate for complex industrial FDD and FTC applications[12,16]. The general structure for an integrated fault-tolerant MPC is described in Figure 1 along with common fault types. Similar structures have been discussed in a number of papers written by Zhang and Jiang[2] and Mhaskar et al. [17,18,19], for example.

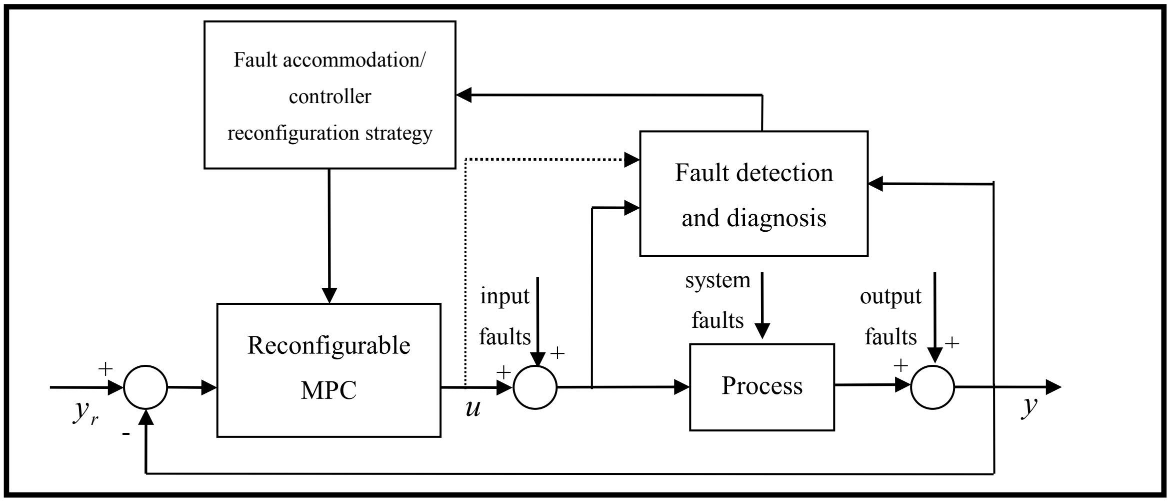

Figure 1. Schematic diagram for an active fault-tolerant MPC.

2.1.1 PLS-based fault accommodation FTC strategy for analyser and sensor faults

The fault accommodation-based FTC strategy analyses and accommodates MPC inputs, outputs and process parameters based on the fault information and measurement predictions provided by the FDD. In this work, PLS (NIPALS) by Wold et al.[20] is used as an FDD. The NIPALS algorithm is presented in Appendix A.1. The estimations are based on the measurements, controller input signals, actual cascade controller measurements and disturbances relayed to the FDD. The fault accommodation, therefore, effectively masks both the process and the control component from faults through fault residuals, while still taking advantage of both the faulty and the correctly functioning parts of the process.

In the data-based fault accommodation-based FTC, a fault accommodation block is used to accommodate the faulty input and output measurements. This fault accommodation block is set between the nominal controller and the plant. In this block, the faulty input or output measurement is accommodated using the fault estimations from the data-based FDD method.

A data-based FTC strategy is presented for the accommodation of the faulty measurements of the controlled variables (CVs), manipulated variables (MVs) or disturbance variables (DVs). In this example, a dynamic PLS formulation is used to predict the non-faulty measurement values of the faulty CV, MV or DV measurements. A fault accommodation block, based on a dynamic PLS algorithm, is set between the plant and the nominal controller. This fault accommodation block uses historical process data to predict the measurement values from the input values u, the output values of y or the disturbance values of d; and the past process output values y_{past}, input values u_{past} or disturbance values d_{past}. If necessary, the faulty CV, MV or DV measurement can be accommodated in order to prevent the effects of the faults on the target process. The fault accommodation block for the CV is presented in Figure 2; for the MV in Figure 3; and for the DV in Figure 4.

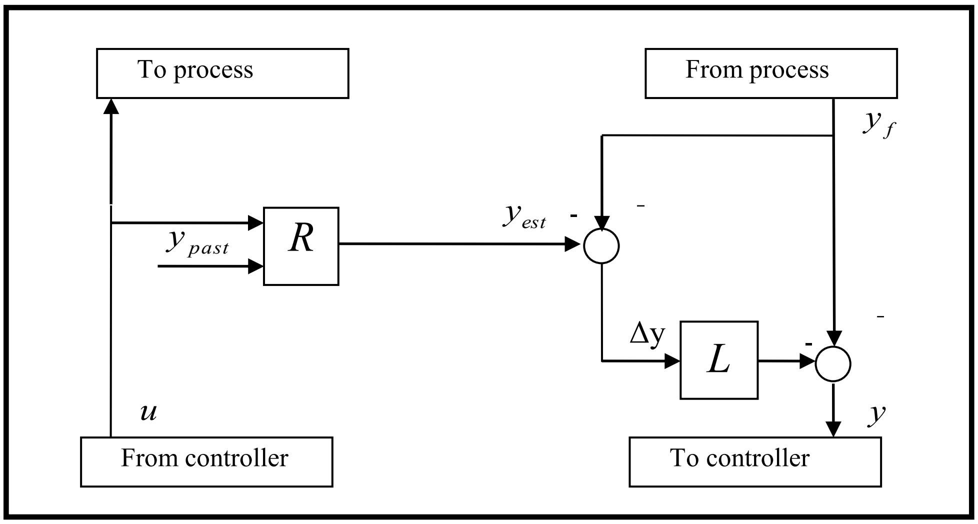

Figure 2. The data-based fault accommodation block with faulty input vector y_f and accommodated CV measurement y.

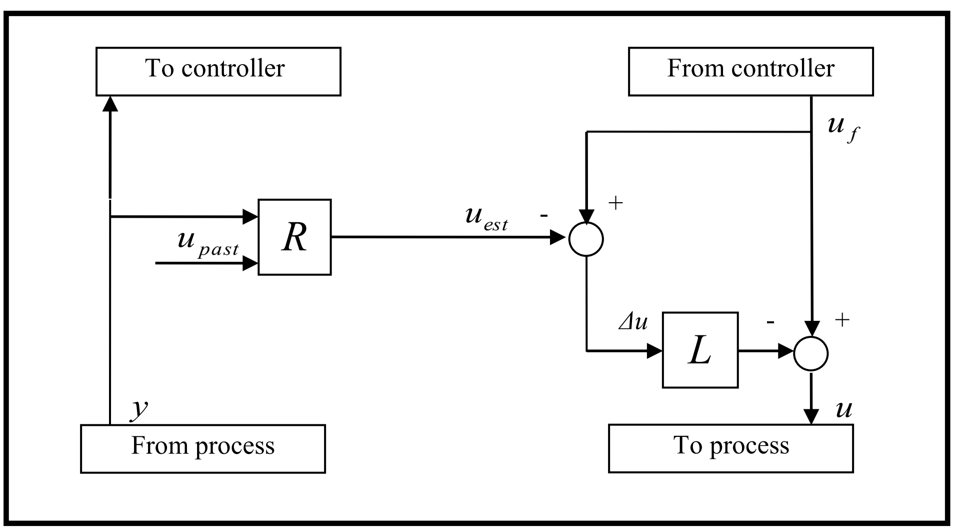

Figure 3. The data-based fault accommodation block with faulty input vector u_f and accommodated MV measurement u.

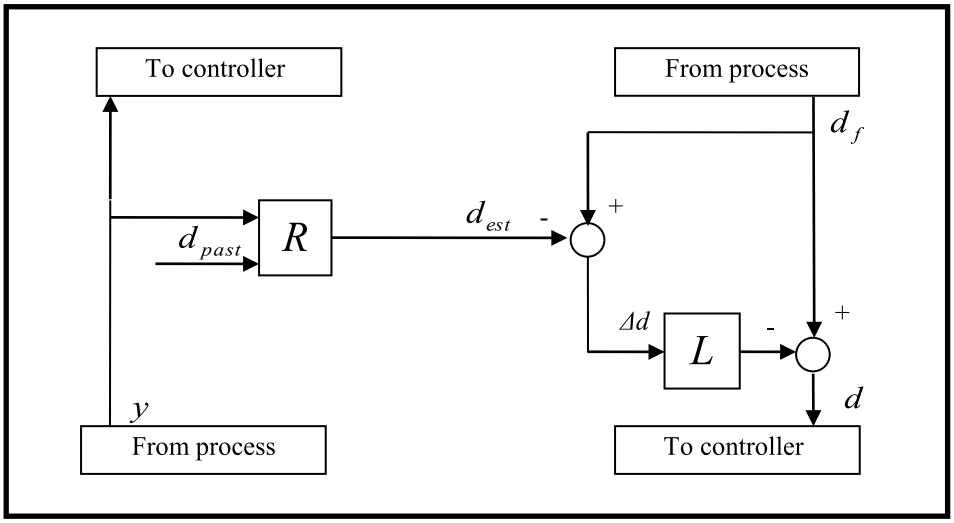

Figure 4. The data-based fault accommodation block with faulty disturbance vector d_f and accommodated DV measurement d.

In the following, the PLS regression for y_{est}, u_{est} and d_{est} are represented with variable v_{est} for each case. In the figures, L is the parameter matrix affecting the degree of fault accommodation based on the probability of the fault. If no fault is detected, the probability of the fault is zero and the L matrix is set to a zero matrix. When a fault is detected, the probability of the fault is increased during each time step and the L matrix is adjusted accordingly to increase the degree of the accommodation.

L is the dependant of the period of time the fault has been detected: the longer the time, the higher the L matrix diagonal value corresponding to the faulty variable, finally ending up to a value of 1 in the diagonal entry of the faulty variable, which allows full accommodation of the faulty measurement. If a fault is detected, the procedure increases the fault probability counter by one; however, if the delay counter is over the min limit, the FTC actions are initiated. The values of the ith diagonal entry of the parameter matrix L is calculated by using the following equation:

$$L_i = \frac{c_{i,t} - c_{i,\min}}{c_{i,\max} - c_{i,\min}}, c_{i,t} \geq c_{i,\min}, \; c_{i,t} \leq c_{i,\max} \qquad (1)$$

where $c_{i,t}$ is the value of the fault probability counter of the ith diagonal entry at the time step t, $c_{i,max}$ is the maximum value of the ith fault probability counter, and the $c_{i,min}$ is the minimum limit for the fault detection of the ith sensor. During each time step when a fault is detected, the value of $c_{i,t}$ is increased by one until the value of the counter reaches $c_{i,max}$; accordingly, during each time step when no fault is detected, the counter $c_{i,t}$ is decreased by one until the value of the counter falls below $c_{i,min}$, after which the accommodation of the ith measurement is stopped.

The fault estimation is carried out by using PLS regression based on the set of process data. The input matrix to the PLS regression matrix R in each case are the inputs u, the current measurements y, the disturbances d and the past values y_{past}, u_{past} and d_{past}.

$$v_{est} = XR \tag{2}$$

where X is the PLS input data matrix with the past values of y, u or d and the input values u, the current measurements y, or the disturbances d and R is the PLS regression matrix:

$$R = WQ \tag{3}$$

where W is the weight matrix of the input matrix X, and Q the loadings of y or u, which are estimated from process data with the nonlinear iterative partial least squares (NIPALS) algorithm[20] that is presented in Appendix A.1. The difference between v_{est} and v_f, Δv, is then measured:

$$\Delta v = v_f - v_{est} \tag{4}$$

The root mean square error of the prediction (RMSEP) index between the estimated and the measured value is monitored. This index is presented in the following equation:

$$RMSEP = \sqrt{\frac{\sum_{i=1}^{n} (\hat{v}_i - v_i)^2}{n}} \tag{5}$$

where n is the number of samples in the test data set. Variable v is u, y or d, depending on which variable is monitored. Based on the RMSEP value, the fault detection threshold is determined empirically by minimising the false alarm rate while attempting to maximise the detection of the actual faults at the same time. If the RMSEP value is greater than the set threshold value, then the probability of the fault and the cell value of matrix L corresponding to the faulty variable is increased. The accommodated measurement can then be acquired through:

$$v = v_f - L\Delta v \tag{6}$$

where Δv is the residual between the faulty value and the predicted value, and v is either y, u or d, depending on which variable is monitored. As a result, the following equation describes the total accommodation of the faulty measurement $v_{f,i}$ during the time instant of i to a healthy measurement v_i by using process data and PLS regression:

$$v_i = v_{f,i} - L(v_{f,i} - X_i WQ) \tag{7}$$

where PLS input data matrix X_i contains either u or y at the time instant of i and recursive inputs y_{past}, u_{past} or d_{past}, W is the weights of v, Q is the loadings of v and L is the parameter matrix controlling the degree of accommodation.

2.1.2 Controller reconfiguration-based FTC for MV sensor and actuator faults

A controller reconfiguration-based FTC component relies on adjusting the controller itself directly by changing the controller structure, models or parameters. In fact, the pure reconfiguration-based strategy (restructurization) only uses the correctly functioning part of the system for control purposes. One way of handling the controller reconfiguration with MV sensor or actuator faults is control allocation (CA) and the 'Daisy-chaining principle' (DCP)[21,22]. In the DCP, a set of actuators are defined as the primary actuators and the second set of controllers as the secondary actuators. If some of the first set of actuators reaches saturation, caused by an actuator failure for example, then the secondary actuators are used for control thereby preventing the faults from affecting the controlled variables. The most important factor in using CA for FTC is that it can deal directly with total actuator failures without actually requiring controller reconfiguration or accommodation[23]. The FTC, based on controller reconfiguration, can be further improved with an active FDD component providing the controller with fault information as soon as it is detected so that the controller configuration can be changed before the fault can affect the controller's performance[24].

A method based on the controller reconfiguration approach for MV sensor and actuator faults is presented next. To be able to apply control allocation to a process controlled by an MPC, there should be sufficient redundancy in the target process in order to allow compensation of the faulty control variables. This can be accomplished, for instance, by replacing the faulty manipulated variable with a measured, but also controllable disturbance variable, the input to output model of which is available in the MPC. In essence, this FTC approach requires an availability of an auxiliary MV in the target process that can be used to compensate for the faulty MV. In this study, this auxiliary MV is treated as a DV and set as an MV in case of a fault in an MV.

The detection of an MV sensor failure was presented in the previous section. The failure of an actuator is detected by calculating the root mean square error (RMSE) index from actual measurements and the reference trajectory set by the MPC, and comparing the index value to a detection threshold. This index is presented in the following equation:

$$RMSE = \sqrt{\frac{\sum_{i=1}^{n} \left(u_{ref,i} - u_i\right)^2}{n}} \tag{8}$$

where n is the number of measurements, u_{ref} the input reference given by the MPC, and u is the measured MV value. As with the RMSEP threshold, the fault detection threshold is determined empirically by minimising the false alarm rate while attempting to maximise the detection of actual faults at the same time.

The scheme for a controller reconfiguration-based FTMPC is presented in Figure 5. The figure contains the controlled variable matrix CV, the manipulated variable matrix MV and the measured disturbance matrix DV. In addition, the selected controlled variable measurements y_{CV}, references for the controlled variables y_r, the selected measured disturbance values y_{DV} and the selected control inputs u_{MV} are presented in the figure

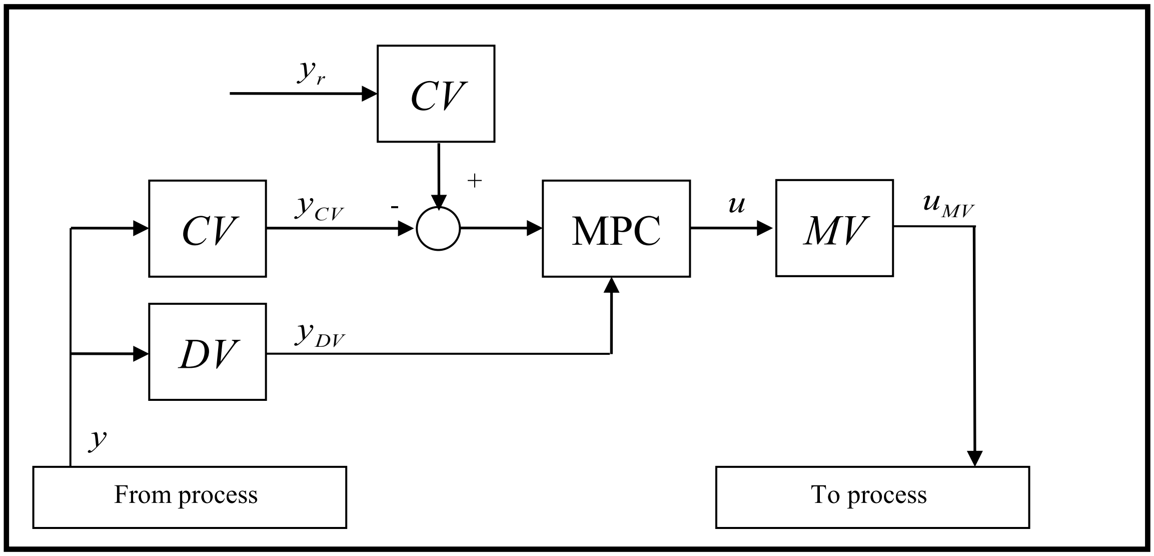

Figure 5. Structure of an MPC with the variable determination matrices *CV*, *MV* and *DV* and an MPC component for optimising the future output.

If the RMSE (for MV actuator faults) value of u_i has been over the detection threshold for a sufficiently long period, a controller reconfiguration action is carried out: the control configuration of the nominal controller is changed by adjusting matrix *MV* and matrix *DV*. In essence, in the case of a fault in the *i*th *MV*, the diagonal entry *i* of matrix *MV* is set to zero and the *i*th diagonal entry of matrix *DV* is set to 1, thereby effectively setting the flow measurement of the faulty actuator as a measured disturbance. In order to compensate for the loss of an *MV*, the measured disturbance u_j is set as an *MV* by setting diagonal entry $K+j$ of the matrix *MV* as the value 1 and diagonal entry $K+j$ in the matrix *DV* to zero.

A similar approach can be applied for MV sensor faults. The controller reconfiguration of an MV is carried out if the RMSEP index crosses the determined detection threshold. If a fault is detected, the faulty MV is moved in the opposite direction of the fault by the amount of PLS-based fault estimation, after which the faulty MV reconfiguration is carried out.

2.1.3 The integrated fault-tolerant model predictive controller

To conclude, the active, data-based integrated FTMPC contains a nominal MPC, an FDD method for the fault diagnosis purposes and the fault accommodation and controller reconfiguration FTC methods for reducing the faults' effects in a process affected by time-delays and process disturbances. The delays between the variables are taken into account by selecting the input data to the FDD and FTC based on the delays. For instance, to predict the value of the CV y during the current time step, the value of the input variable u is taken d time steps from the past, where d is the delay between variables u and y.

The FTMPC is divided into three active FTC strategies that reduce the effects of different fault types. The fault types to be countered are the sensor or, for example, process analyser faults (drift- or bias-shaped faults) for the CVs, DVs and MVs and MV actuator faults. The first FTC strategy is based on the fault accommodation FTC method and on the recursive, NIPALS-based PLS for the sensor and, for example, process analyser faults in the CVs or DVs. The second FTC strategy uses the recursive, NIPALS-based PLS and the fault accommodation and controller reconfiguration FTC methods for the sensor faults in the MVs. The third FTC strategy utilises the controller reconfiguration FTC method for the MV actuator faults. These strategies are explained in detail in Appendix D and the integrated fault-tolerant MPC is presented in Figure 6. In this figure, $y_{CV+DV+MV}$ contains measurements for the CVs, DVs and MVs; f_1, f_2 and f_3 contain the fault diagnosis information for each of the FTC strategies; $L_{\Delta yCV+DV}$ contains the corrections for the CV and DV measurements; $L_{\Delta uMV+DV}$ contains the correction values for the MV outputs of the MPC; $MV+DV$ contains the matrices for the MPC to determine which of the MVs and DVs are used as MVs should the controller reconfiguration action occur.

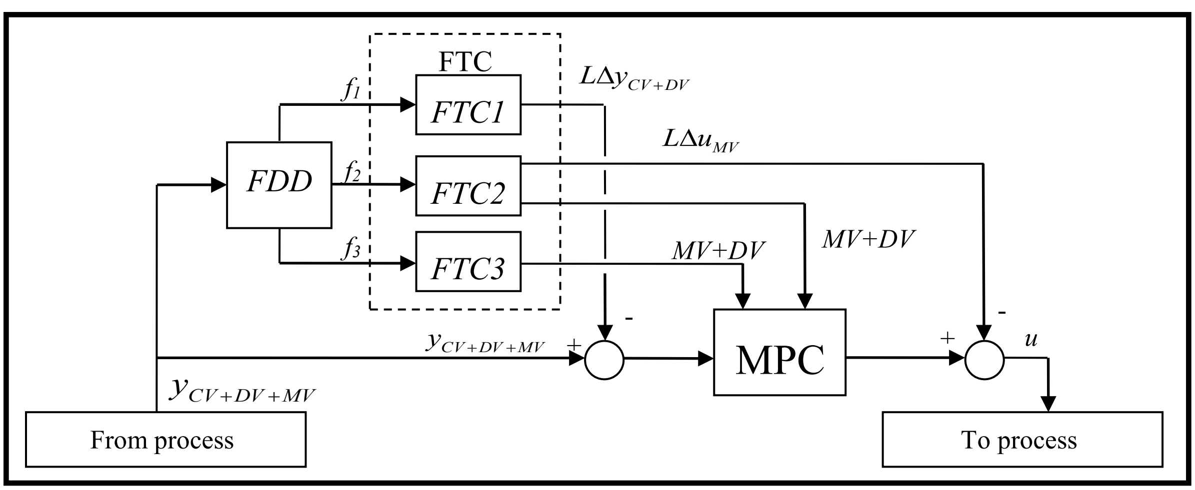

Figure 6. The integrated FTMPC with three FTC strategies.

3 Application to an industrial dearomatization process

The target process for implementing the data-based fault-tolerant MPC is a complex dearomatization process, LARPO (acronym of Finnish term ‘Liuottimien ARomaattien POisto’), located at Neste Oil’s Naantali refinery, Finland. The purpose of the dearomatization process is to remove aromatic compounds from the solvent feedstock through catalytic hydrogenation in a continuous process. Exothermic saturation reactions take place in the reactors, which remove the aromatic compounds from the feed. The product quality parameters, such as the initial boiling point or flashpoint, are adjusted in the distillation part of the unit. LARPO is in a crucial position in the Naantali refinery because most of the solvent products of the refinery are non-aromatic, and a failure in the product quality analysers may cause large quantities of off-spec products and thus significant financial losses. Potentially, a low-quality end product may also have an effect on customers and cause problems in selling the final products.

The LARPO dearomatization process is composed of two trickle-bed reactors with packed catalyst beds for removing the aromatic compounds; a distillation column used for controlling the specifications of the end products; several heat exchangers for importing and exporting energy in the process; separation drums; a filling plate stripper; and several other pieces of process equipment that carry out supplementary tasks in the unit. The flow diagram of the LARPO dearomatization process is presented in Figure 7[25].

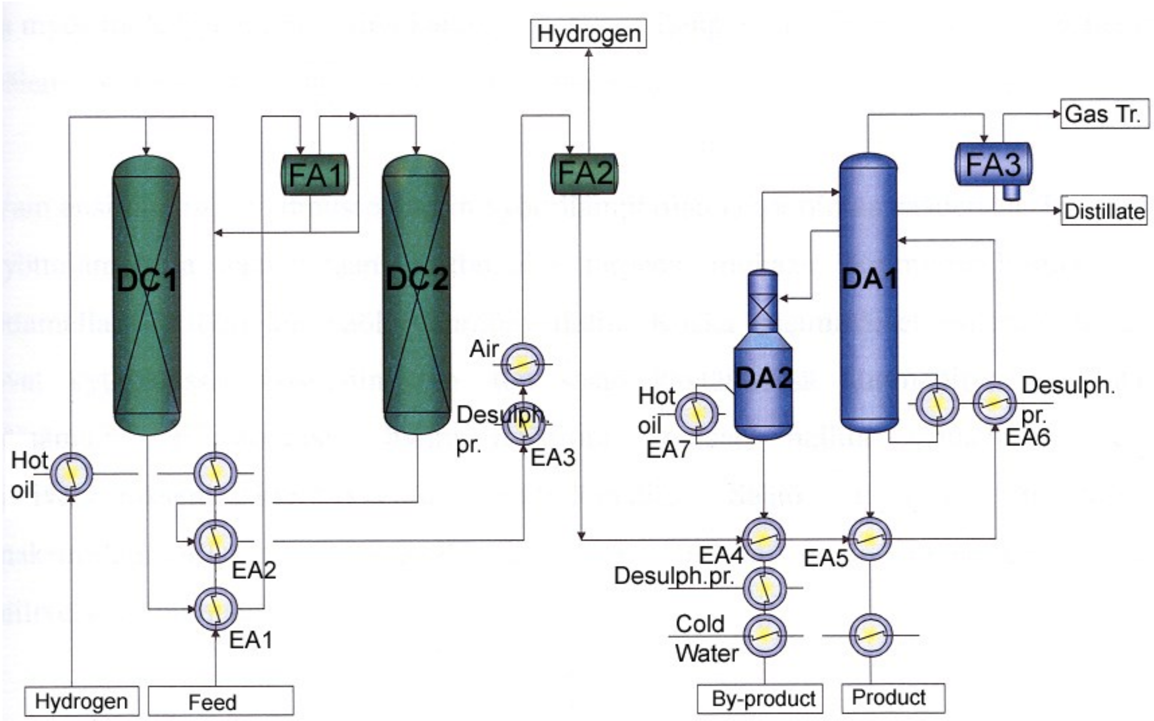

Figure 7. The industrial dearomatization process, LARPO, at the Naantali refinery[25].

3.1 Control of the target process

The primary control objective for the MPC of the LARPO dearomatization process is to keep the distillation column DA1 bottom product above the product quality limit. A secondary objective is to minimise the additional production costs by aiming to keep the product quality as close as possible to the specifications, while maximising the feed rate. In practice, the goals are to maintain the column DA1 bottom product within specifications (initial boiling point, flashpoint or column DA1 temperature), and to minimise the stripper unit DA2 bottom product flashpoint within the by-product specification limits.

In the measurements of both the distillation column DA1 and the stripper unit DA2 bottom products, the product quality should never fall below the minimum specification limits. If the quality specifications are not met, off-spec production occurs and an over-quality product needs to be mixed with the off-spec product in order to meet the specifications. However, if the value of the variables is higher than the minimum limit, energy and financial losses increase because a larger amount of valuable product goes for reprocessing with the overhead distillate flow.

3.2 Variables of the target process

Five controlled variables are defined for the MPC of the LARPO dearomatization process: column DA1 bottom product initial boiling point (DA1_BP_IBP); DA1 bottom product flashpoint (DA1_BP_FP); DA1 liquid distillate flow rate (DA1_DIST_FC); DA1 pressure-compensated temperature (DA1_TC); and column DA2 bottom product flashpoint (DA2_BP_FP). The controlled variables and the individual control targets for these variables are presented in Table 1.

Of these controlled variables, DA1_BP_IBP, DA1_BP_FP and DA1_TC are alternative variables and thus only one of these can be used at a time for control. Only DA1_BP_FP is relevant to the specific heavy feedstock studied in this work. The overhead flow rate DA1_DIST_FC is minimised by controlling the by-product flashpoint DA2_BP_FP thus maximising the flow to the by-product stripper unit DA2 while minimising the overhead flow rate DA1_DIST_FC.

Table 1. The LARPO controlled variables.

Variable name	Variable description	Unit
DA1_BP_IBP	DA1 bottom product initial boiling point *(target)*	*°C*
DA1_BP_FP	DA1 bottom product flashpoint *(target)*	*°C*
DA1_DIST_FC	DA1 liquid distillate flow *(minimise indirectly)*	*kg/h*
DA1_TC	DA1 pressure-compensated temperature *(target)*	*°C*
DA2_BP_FP	DA2 bottom product flashpoint *(target, minimise)*	*°C*

Four disturbance variables are used in the MPC: the DA1 feed flow rate (DA1_FEED_FC); the DA1 feed temperature (DA1_FEED_TC); the DA1 heating medium temperature (DA1_HEAT_TC); and the DA1 pressure (DA1_PC). The disturbance variables and are presented in Table 2.

Table 2. The LARPO disturbance variables.

Variable name	Variable description	Unit
DA1_FEED_FC	DA1 feed flow rate	*t/h*
DA1_FEED_TC	DA1 feed temperature	*°C*
DA1_HEAT_TC	DA1 heating medium temp.	*°C*
DA1_PC	DA1 Pressure	*kPa*

Four manipulated variables are used for the control of the process: the DA1 reflux flow rate (DA1_REFLUX_FC); the EA6 hot stream feed rate (DA1_EA6_FEED_FC); the DA2 feed flow rate

(DA2_FEED_FC); and the EA7 hot stream feed rate (DA2_EA7_FEED_FC). The manipulated variables are presented in Table 3.

Table 3. The LARPO manipulated variables.

Variable name	Variable description	Unit
DA1_REFLUX_FC	DA1 reflux flow rate (*maximise*)	*t/h*
DA1_EA6_FEED_FC	EA6 hot stream feed rate (*minimise*)	*t/h*
DA2_FEED_FC	DA2 feed flow rate (*maximise*)	*t/h*
DA2_EA7_FEED_FC	EA7 hot stream feed rate (*keep steady*)	*t/h*

3.3 MPC parameters

The MPC parameters are adjusted according to the dynamics of the simulated dearomatization process. The control cycle for the MPC is set to one minute, since the changes in the process are relatively small and there is no need for faster control. The prediction horizon is set long enough to be able to react as early as possible to most situations in the simulated process. Since the total delays - including the analyser delays in the process - vary between 0-40 minutes, the prediction horizon is set to 50 minutes. This means that while the prediction horizon is longer than the largest delay, it is not too long to keep the process under control. The control horizon is set to 40 minutes, which is a good compromise between the efficiency and the required computation time.

The primary controlled variable (DA1_BP_IBP, DA1_BP_FP or DA1_TC) weights are set to 10 to indicate that the main column bottom product is to be kept at the setpoint at all times. The weight for the secondary variable DA2_BP_FP is set to 1 to indicate that the minimisation of the by-product flashpoint is not as important as keeping the main product within the defined specifications.

The constraints for the CVs are set according to the product specifications and to keep the MPC within control range. The CV weights and the constraints for the CVs are presented in Table 4 .

The maximum constraints for the MVs are set according to the mechanical limits of the target controller and the minimum constraints are set according to the operational limits; for instance, DA2_FEED_FC has a non-zero minimum value in order to ensure flow to the side stripper. Also, DA1_REFLUX_FC would need to have a minimum flow back to the column in order to keep the column separating capacity at moderate levels. DA1_EA6_FEED_FC has a minimum limit of 40% of the maximum limit since there is a minimum level of reboiling required for the separation procedure. Furthermore, if there would not be enough energy available, there would not be enough feed for side stripper DA2.

In Table 4 and Table 5, the minimum constraints are presented as absolute values for the CVs and as percentages of the maximum constraint for the MVs. The minimum value of the setpoint (of the minimum constraint) is also presented in Table 4.

The MV change rate constraints are set to -5% and +5% of the range of variation allowed for the controller. The weights for the input variables are set to 0, allowing full freedom for the input variables; in essence, this leaves the input variables out of the MPC objective function. The weights for the MV rates are set at 5. Selecting this value allows a relatively fast response time for each MV, the selection being based on the control performance. The constraints and weights for the manipulated variables are presented in Table 5.

Table 4. The constraints, weights and minimum setpoint values of the CVs.

CVs:	Constraints % of the max limit		Weights	Min setpoint (of the min limit)
	Min	Max		
DA1_BP_IBP	219,0	245,0	1	+0.5%
DA1_BP_FP	79,8	100,0	1	+0.5%
DA1_DIST_FC	-	-	-	-
DA1_TC	261,5	275,0	1	+0.5%
DA2_BP_FP	66,0	80,0	1	+0.5%

Table 5. The constraints and weights of the MVs.

MVs:	Constraints % of the max limit		Rate constraints % of the range of variation		Weights	Rate weights
	Min	Max	Min	Max		
DA1_REFLUX_FC	25,0%	100,0%	-5,0%	+5,0%	0	5
DA1_EA6_FEED_FC	40,0%	100,0%	-5,0%	+5,0%	0	5
DA2_FEED_FC	25,0%	100,0%	-5,0%	+5,0%	0	5
DA2_EA7_FEED_FC	15,0%	100,0%	-5,0%	+5,0%	0	5

3.4 Faults in the target process

In this section, faults in the target process are presented; further, the fault types taken into account in the simulation study part are also discussed. In a study carried out by Liikala[26], Naantali refinery's process diary and process history were examined in order to gather specific information on the faults in the dearomatization process. During the time period covered by the study, nearly 70% of all faults in the LARPO unit were related to analysers as shown in Figure 8.

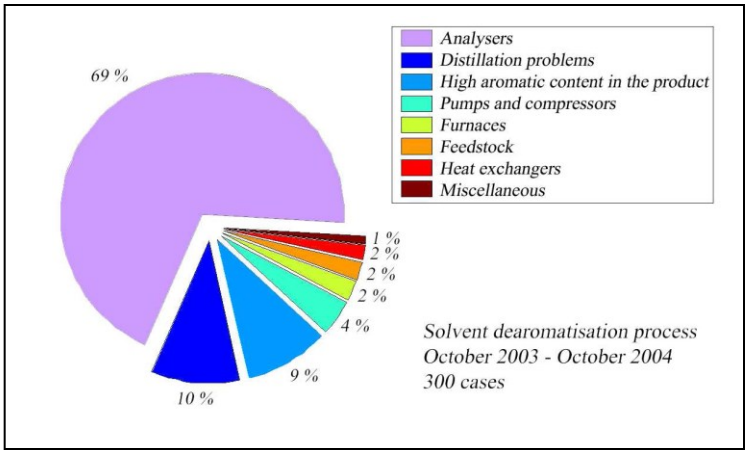

Figure 8. Most common faults in the dearomatization process during one year of operation[26].

To obtain more information on the faults and their effects to the process, data from the Naantali refinery maintenance department were studied over the period 09/2008-09/2009 by the authors. During this period, faults such as temperature, flow and pressure measurements, control valves and process analysers were taken into account. All faults requiring maintenance work were included in the study. The fault data were divided into three categories: analyser faults, measurement device faults and control valve faults. Based on the results, 42% of the faults were located in the analysers; 42% in the measurement devices; and 16% in the control valves. The results are shown in Figure 9.

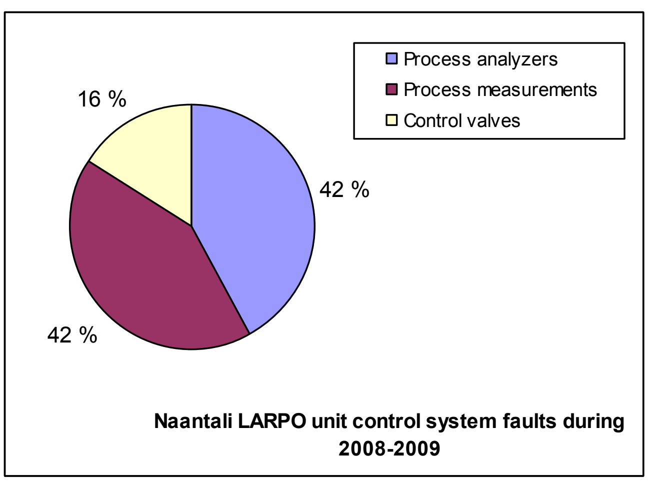

Figure 9. Naantali LARPO unit control system faults during 09/2008–09/2009.

In addition to data from the maintenance department, the flashpoint analyser output on a heavy grade feed run was also compared to the laboratory measurements during the period 09/2008–09/2009. The analysis used to measure the flashpoint is EN ISO 2719-2002 M, which has a repeatability of 2.8°C on the given data set. The aim of the comparison was to determine the number of measurement points in which the analyser measurement differs from that of the laboratory by more than 2.8°C which, in practice, means that the analyser measurement is faulty. In addition, the downward faults causing off-spec and upward faults resulting in over-quality products were also categorised. Based on the data, off-spec was produced due to the analyser readings in 3% of the cases; too high a quality product was also produced in 3% of the cases. In total, 6% of the analyser measurements during the heavy grade run differed by more than 2.8°C from those of the laboratory, causing either off-spec production or too high quality production.

Based on these studies, it can be concluded that most of the faults in the LARPO unit are located in process analysers, although some faults also occur in other measurements and control valves of the unit. The fault types that were tested with the final FTC strategy were narrowed down to a stuck valve fault for the actuators, bias- and drift-shaped faults for analysers and sensors of controlled variables, and bias-shaped faults for the sensors of disturbance and manipulated variables.

3.5 Testing environment

The simulation studies on the LARPO dearomatization process were carried out in the ProsDS (formerly known as PROSimulator) - a dynamic process simulator developed by Neste Jacobs Oy - which has simulation models representing the physical-chemical behaviour of the target process.

The simulation model for the LARPO unit contains a large number of measurements, analyser readings and low-level control loops in order to accurately present the behaviour of the target process. An accurate model thus enables the testing and development of different control strategies offline.

The measurements from the ProsDS were transferred in real time to the Matlab workspace, from where the measurements were further transferred to the Matlab software platform. The platform handles the orchestration and pre-treatment of data. Pre-treatment includes noise and outlier removal by filtering, and data interpolation for the missing data points.

4 Results and economic evaluation

In order to demonstrate the effectiveness of the proposed FTC strategy, an FTC application for a simulated dearomatization process was implemented. The simulation results with different fault types are presented in this section of the paper and the results are summarised. The effectiveness of the developed FTC strategy is measured by the response time and the magnitude of the disturbance caused to the target process variables.

4.1 The structure of the models for the FTC strategies

In this section, the model structures for different FTC strategies are presented.

The structure of the PLS models used in the FTC strategy of the CVs is presented in Table 6 for the 1st set of PLS models (used for detecting the faults), and the 2nd set of PLS models (used for identifying the magnitude of the faults). These sets of variables differ by the recursive elements, which are delayed more in the 2nd set than in the 1st set. These recursive elements for both of the models are presented with a gray background. The structure of the PLS model for the FTC strategy for DV sensors is presented in Table 7 for the 1st and 2nd sets of models. Again, these sets of variables differ by the recursive elements, which are delayed more in the 2nd set than in the 1st set. These recursive elements for both of the models are presented with a gray background. The PLS model structure for the MV sensors is presented in Table 8.

Table 6. The structure of the 1st and 2nd PLS models for the FTC strategy for the CV sensor faults.

Model	PLS_1	PLS_2	PLS_3	PLS_4	PLS_5
Output	DA1_BP_IBP	DA1_BP_FP	DA1_DIST_FC	DA1_TC	DA2_BP_FP
Inputs	DA1_FEED_FC	DA1_FEED_FC	DA1_FEED_FC	DA1_FEED_FC	DA1_FEED_FC
	DA1_FEED_TC	DA1_FEED_TC	DA1_FEED_TC	DA1_FEED_TC	DA1_FEED_TC
	DA1_HEAT_TC	DA1_HEAT_TC	DA1_HEAT_TC	DA1_HEAT_TC	DA1_HEAT_TC
	DA1_PC	DA1_PC	DA1_PC	DA1_PC	DA1_PC
	DA1_REFLUX_FC	DA1_REFLUX_FC	DA1_REFLUX_FC	DA1_REFLUX_FC	DA1_REFLUX_FC
	DA1_EA6_FEED_FC	DA1_EA6_FEED_FC	DA1_EA6_FEED_FC	DA1_EA6_FEED_FC	DA1_EA6_FEED_FC
	DA2_FEED_FC	DA2_FEED_FC	DA2_FEED_FC	DA2_FEED_FC	DA2_FEED_FC
	DA2_EA7_FEED_FC	DA2_EA7_FEED_FC	DA2_EA7_FEED_FC	DA2_EA7_FEED_FC	DA2_EA7_FEED_FC
1st model	DA1_BP_IBP($t-d_1$)	DA1_BP_FP($t-d_1$)	DA1_DIST_FC($t-d_1$)	DA1_TC($t-d_1$)	DA2_BP_FP($t-d_1$)
	DA1_BP_IBP($t-d_2$)	DA1_BP_FP($t-d_2$)	DA1_DIST_FC($t-d_2$)	DA1_TC($t-d_2$)	DA2_BP_FP($t-d_2$)
2nd model	DA1_BP_IBP($t-d_3$)	DA1_BP_FP($t-d_3$)	DA1_DIST_FC($t-d_3$)	DA1_TC($t-d_3$)	DA2_BP_FP($t-d_3$)
	DA1_BP_IBP($t-d_4$)	DA1_BP_FP($t-d_4$)	DA1_DIST_FC($t-d_4$)	DA1_TC($t-d_4$)	DA2_BP_FP($t-d_4$)

Table 7. The structure of the 1st and 2nd PLS models for the FTC strategy for the DV sensor faults.

Model	DV_PLS_1	DV_PLS_2	DV_PLS_3	DV_PLS_4
Output	DA1_FEED_FC	DA1_FEED_TC	DA1_HEAT_TC	DA1_PC
Inputs	DA1_TEMP_1	DA1_TEMP_1	DA1_TEMP_1	DA1_TEMP_1
	DA1_TEMP_2	DA1_TEMP_2	DA1_TEMP_2	DA1_TEMP_2
	DA1_TEMP_3	DA1_TEMP_3	DA1_TEMP_3	DA1_TEMP_3
	DA1_OVHD_FLOW_FC	DA1_OVHD_FLOW_FC	DA1_OVHD_FLOW_FC	DA1_OVHD_FLOW_FC
1st model	DA1_FEED_FC($t-d_{max}-d_1$)	DA1_FEED_TC($t-d_{max}-d_1$)	DA1_HEAT_TC($t-d_{max}-d_1$)	DA1_PC($t-d_{max}-d_1$)
	DA1_FEED_FC($t-d_{max}-d_2$)	DA1_FEED_TC($t-d_{max}-d_2$)	DA1_HEAT_TC($t-d_{max}-d_2$)	DA1_PC($t-d_{max}-d_2$)
2nd model	DA1_FEED_FC($t-d_{max}-d_3$)	DA1_FEED_TC($t-d_{max}-d_3$)	DA1_HEAT_TC($t-d_{max}-d_3$)	DA1_PC($t-d_{max}-d_3$)
	DA1_FEED_FC($t-d_{max}-d_4$)	DA1_FEED_TC($t-d_{max}-d_4$)	DA1_HEAT_TC($t-d_{max}-d_4$)	DA1_PC($t-d_{max}-d_4$)

Table 8. The structure of the PLS model for the FTC strategy for the MV sensor faults.

Model	MV_PLS_1	MV_PLS_2	MV_PLS_3	MV_PLS_4
Output	DA1_REFLUX_FC	DA1_EA6_FEED_FC	DA2_FEED_FC	DA2_EA7_FEED_FC
Inputs	DA1_TEMP_1	DA1_TEMP_1	DA1_TEMP_3	DA1_TEMP_2
	DA1_TEMP_2	DA1_TEMP_2	DA1_TEMP_4	DA2_DIST_FC
	DA1_TEMP_3	DA1_TEMP_3	DA1_TEMP_5	DA2_BP_TC
	DA1_TEMP_4	DA1_TEMP_4	DA1_TEMP_6	DA2_BP_FC
	DA1_OVHD_FLOW_FC	DA1_TEMP_5	DA1_BP_FC	
	DA2_DIST_FC	DA1_TEMP_6	DA2_BP_TC	
		DA1_OVHD_FLOW_FC	DA2_BP_FC	
		DA1_BP_FC		
		DA1_FEED_EA_FC		
		DA2_BP_TC		
		DA2_BP_FC		

4.2 The cumulative variances of the PLS models for the FTC strategies

The NIPALS algorithm was used for the iterative training of the PLS models used in the FTC for the CV analyser and sensor faults and for the DV and MV sensor faults. The number of latent variables was determined using the ‘knee-in-the-plot’ method, in which the selection of the latent variables is based on the largest drop in the captured variance of the latent variable. The cumulative variances for the input vector X and output vector Y and the number of Latent Variables (LV) of the PLS models are presented in Table 9 for the CV analyser and sensor faults; in Table 10 for DV sensor faults; and in Table 11 for MV sensor faults.

Table 9. The cumulative variances for *X* and *Y*, and the number of LVs for the PLS for the CV analyser and sensor faults.

PLS model	Cumulative variance of *X*	Cumulative variance of *Y*	Number of latent variables
Model 1:			
PLS_1	88	99	5
PLS_2	89	99	5
PLS_3	89	97	5
PLS_4	94	99	5
PLS_5	88	99	5
Model 2:			
PLS_1	86	99	5
PLS_2	89	99	5
PLS_3	83	91	5
PLS_4	93	99	5
PLS_5	84	92	5

Table 10. The cumulative variances for *X* and *Y*, and the number of LVs for the PLS for the DV sensor faults.

PLS model	Cumulative variance of *X*	Cumulative variance of *Y*	Number of latent variables
Model 1:			
DV_PLS_1	81	98	3
DV_PLS_2	83	99	2
DV_PLS_3	99	99	2
DV_PLS_4	99	99	2
Model 2:			
DV_PLS_1	81	98	3
DV_PLS_2	83	99	2
DV_PLS_3	99	100	2
DV_PLS_4	99	99	2

Table 11. The cumulative variances for *X* and *Y*, and the number of LVs for the PLS for the MV sensor faults.

PLS model	Cumulative variance of *X*	Cumulative variance of *Y*	Number of latent variables
MV_PLS_1	98	69	5
MV_PLS_2	93	87	5
MV_PLS_3	99	99	3
MV_PLS_4	90	85	3

4.3 Results of the FTC strategy for CV analyser and sensor faults

The first fault case had an upward bias-shaped fault in the controlled variable DA1_BP_FP with a magnitude of 5% of the nominal value. The value of the CVs was 1°C higher than the specification limit, which left a small window of operation for the FTC before the product goes off the specifications.

The fault was introduced into the DA1 bottom product flashpoint analyser output during the time step T_1 = 15 minutes. The fault lasted for 90 minutes until the time step T_2 = 105 minutes, after which the fault was removed from the process. The PLS-based prediction and the effect of the fault can be seen in Figure 10, which displays the results of the simulation without the FTC on the left and with the FTC on the right. As can be seen from the figure, the fault had the effect that both DA1_BP_FP and DA2_BP_FP were off the specification limits for 90 minutes unless the FTC system was activated, when DA1_BP_FP was off spec only for 10 minutes.

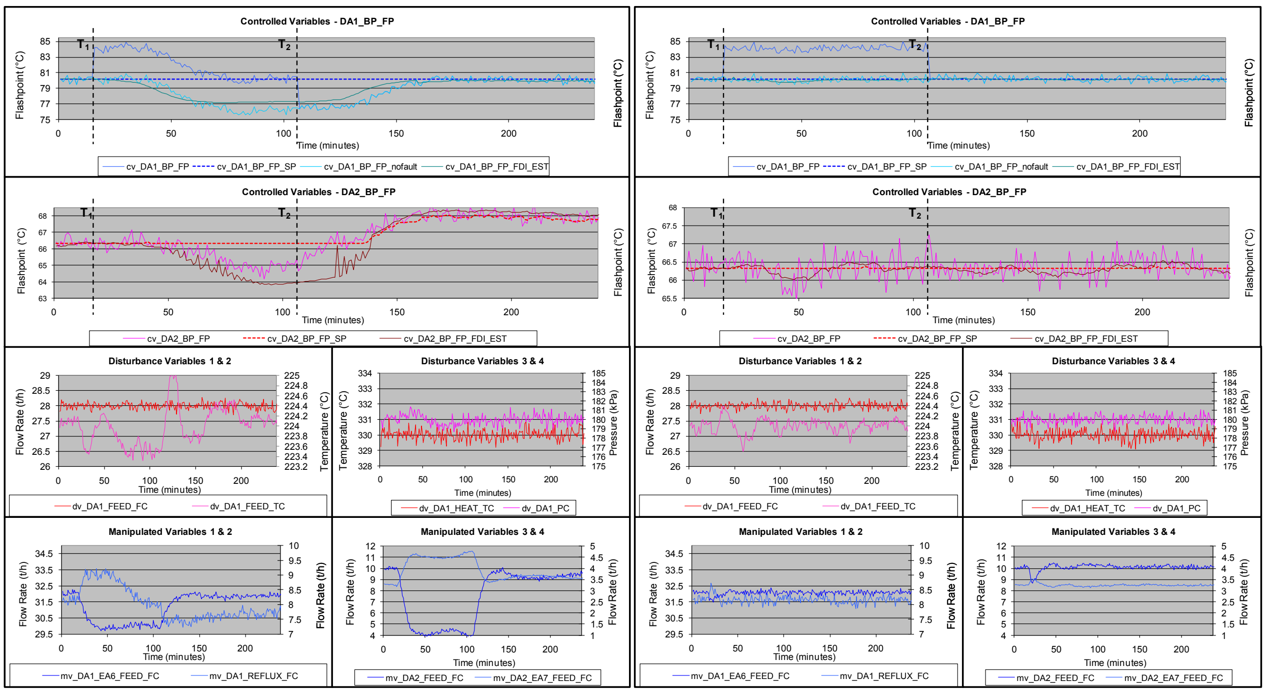

Figure 10. The Effects of a +5% bias faults in the variable DA1_BP_FP during the time step t = 15 - 105 minutes, without the FTC strategy active (left) and with the FTC strategy active (right).

In the second case, the effect of a drift-shaped fault in the CVs was tested with and without the FTC strategy active. An upward drift-shaped gradually-increasing fault with a final magnitude of 5% of the nominal value of the DA1_BP_FP was introduced into the DA1 bottom product flashpoint analyser output, starting from the time step T_1 = 15 minutes. The fault lasted for 90 minutes until the time step T_2 = 105 minutes, after which the fault was removed from the process. The PLS-based prediction and the effect of the fault can be seen in Figure 11. As can be seen from the figure, without the FTC the drift fault had the effect that both DA1_BP_FP and DA2_BP_FP were off the specification limits for 90 minutes and with the FTC, both DA1_BP_FP and DA2_BP_FP remained within the specification limits despite the fault, thus improving the reliability of the control system and providing savings by reducing the amount of off-spec production.

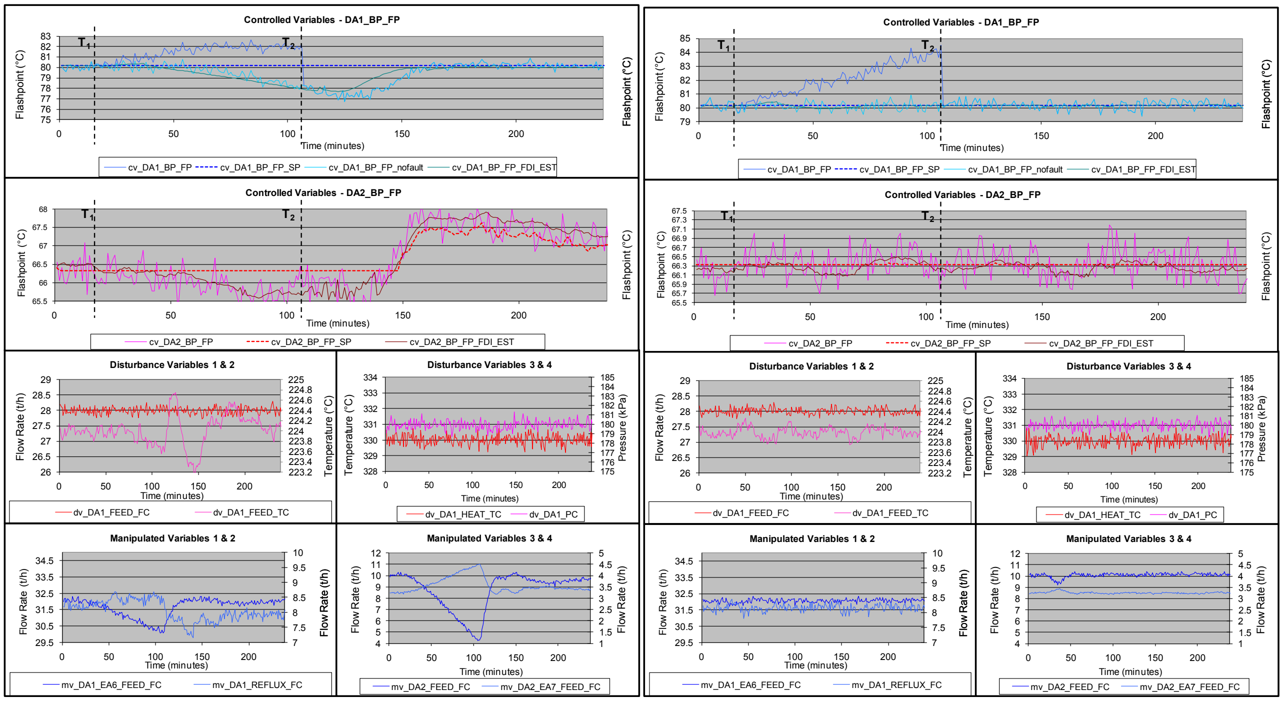

Figure 11. The Effects of a +5% drift fault in the variable DA1_BP_FP during the time step t = 15 - 105 minutes, without the FTC strategy active (left) and with the FTC strategy active (right).

4.4 Results of the FTC strategy for DV sensor faults

The FTC strategy for DV sensor faults was then tested with the bias fault in a DV sensor. A downward bias-shaped fault with a magnitude of 5% of the nominal value of the DA1_FEED_FC was introduced into the DA1 feed flow measurement during the time step T_1 = 15 minutes. The fault lasted for 90 minutes until the time step T_2 = 105 minutes, after which the fault was removed from the target process. The PLS-based prediction and the effect of the fault can be seen in Figure 12. Overall, the fault had the effect that both DA1_BP_FP and DA2_BP_FP were off the specification limits for 90 minutes if the FTC was not active. If the FTC was activated, however, both DA1_BP_FP and DA2_BP_FP remained within the specification limits despite the fault, thus improving the reliability of the control system and reducing off-spec production.

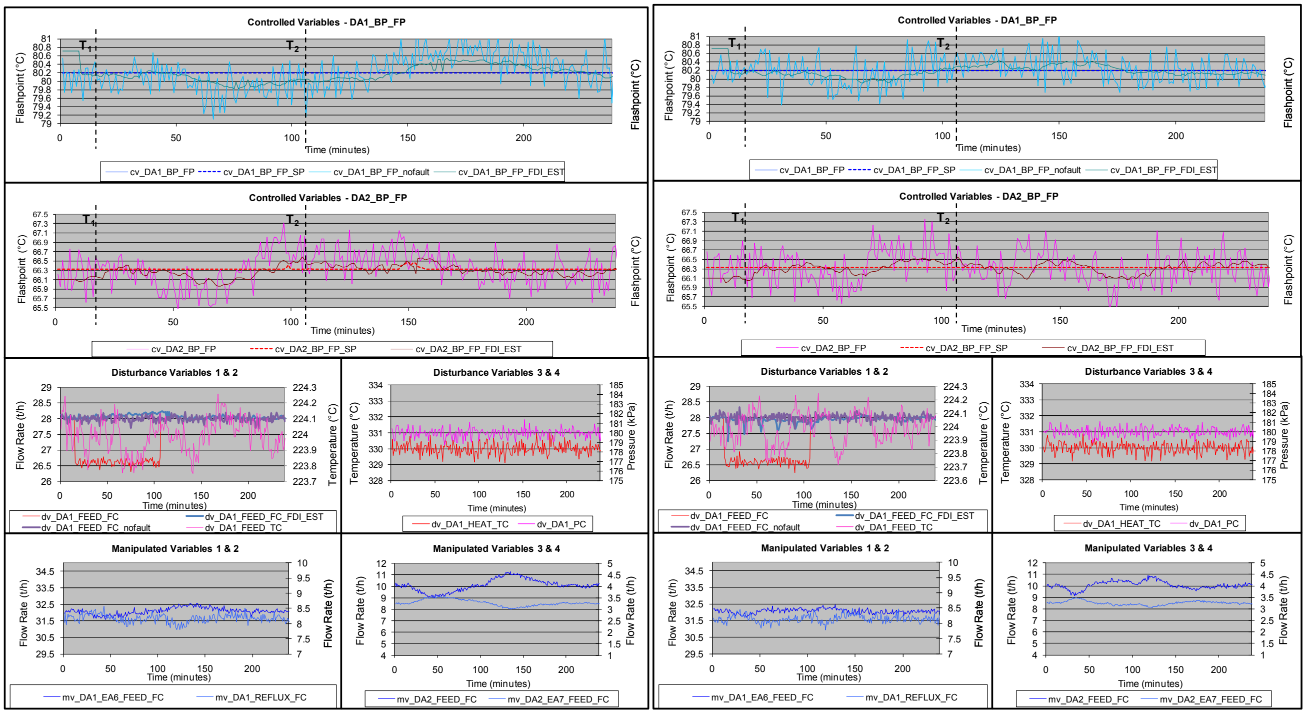

Figure 12. The effects of a -5% bias fault in the variable DA1_FEED_FC during the time step t = 15 - 105 minutes, without the FTC strategy active (left) and with the FTC strategy active (right).

4.5 Results of the FTC strategy for MV sensor faults

The FTC strategy for MV sensor faults was then tested with a bias fault in the MV sensor. A downward bias-shaped fault with a magnitude of 10% of the nominal value of DA1_REFLUX_FC was introduced into the DA1 reflux flow measurement during the time step T_1 = 15 minutes. The fault lasted for 90 minutes until the time step T_2 = 105 minutes, after which the fault was removed from the process. The PLS-based fault estimation and the effect of the fault can be seen in Figure 13. Overall, the fault had the effect that both DA1_BP_FP and DA2_BP_FP were off the specification limits for 40 minutes without the FTC strategy activated. If the FTC strategy was activated, both DA1_BP_FP and DA2_BP_FP remained closer within the specification limits despite the fault, thus improving the reliability of the control system and reducing off-spec production.

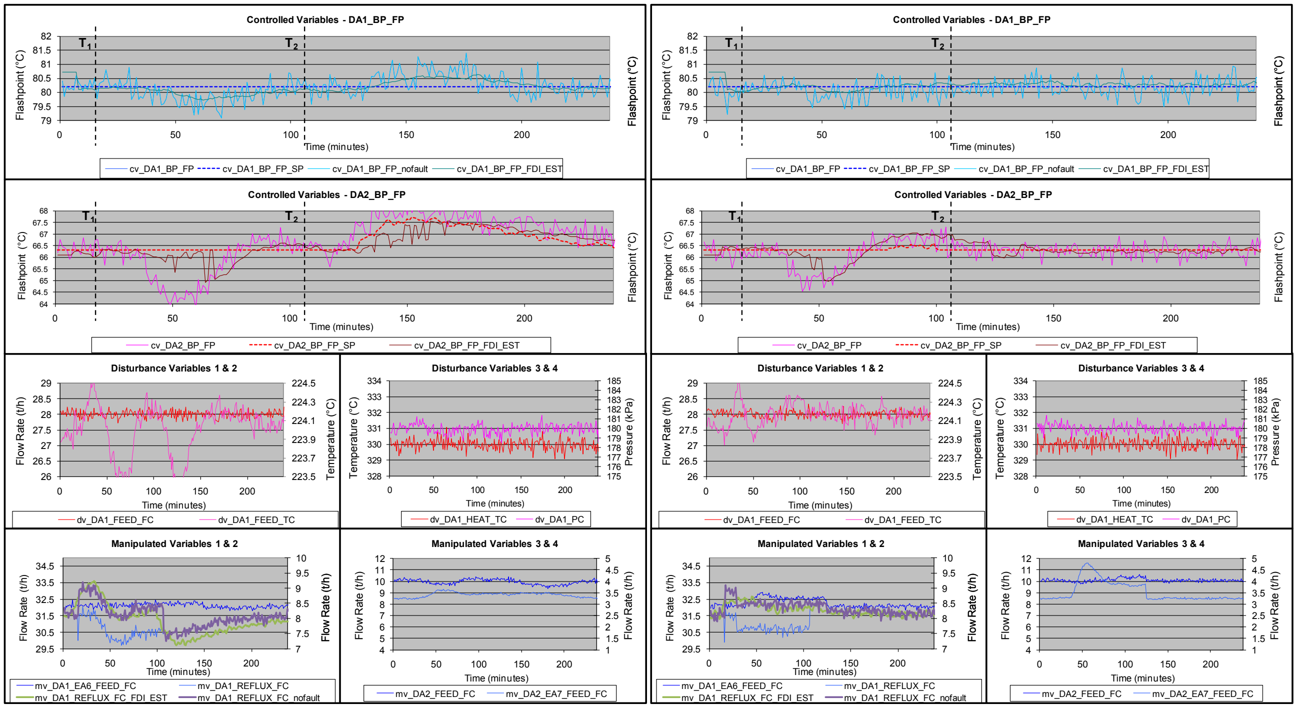

Figure 13. The effects of a -10% bias fault in the variable DA1_REFLUX_FC during the time step t = 15 - 105 minutes, without the FTC strategy active (left) and with the FTC strategy active (right).

4.6 Results of the FTC strategy for MV actuator faults

Finally, the FTC strategy for MV actuator faults was tested. In this case, the stuck valve fault was introduced into the DA2 feed flow measurement during the time step T_1 = 10 minutes. At the same time, a setpoint change of +1% was issued to the DA1 bottom product flashpoint DA1_BP_FP, since under steady state conditions, the stuck valve fault is not detectable; however, if a disturbance or a setpoint change occurs, the fault prevents the valve from being operated, effectively lowering the overall performance of the control system. The FDD component in this case was straightforward: the fault was detected if there was a difference between the control signal and the actuator measurement. The effect of the fault can be seen in Figure 14. Without the FTC activated, the fault caused a delay of 125 minutes in the MPC response, since the MPC could not use the primary controller to change the CV value; eventually, due to the feedback, other MVs had to be used to compensate for the stuck MV. With the FTC activated, the MPC response time was much better: the target setpoint value was reached within 100 minutes after the setpoint change, which was 25 minutes slower than in the case without a stuck valve fault. The FTC strategy thus improved the response time by 100 minutes.

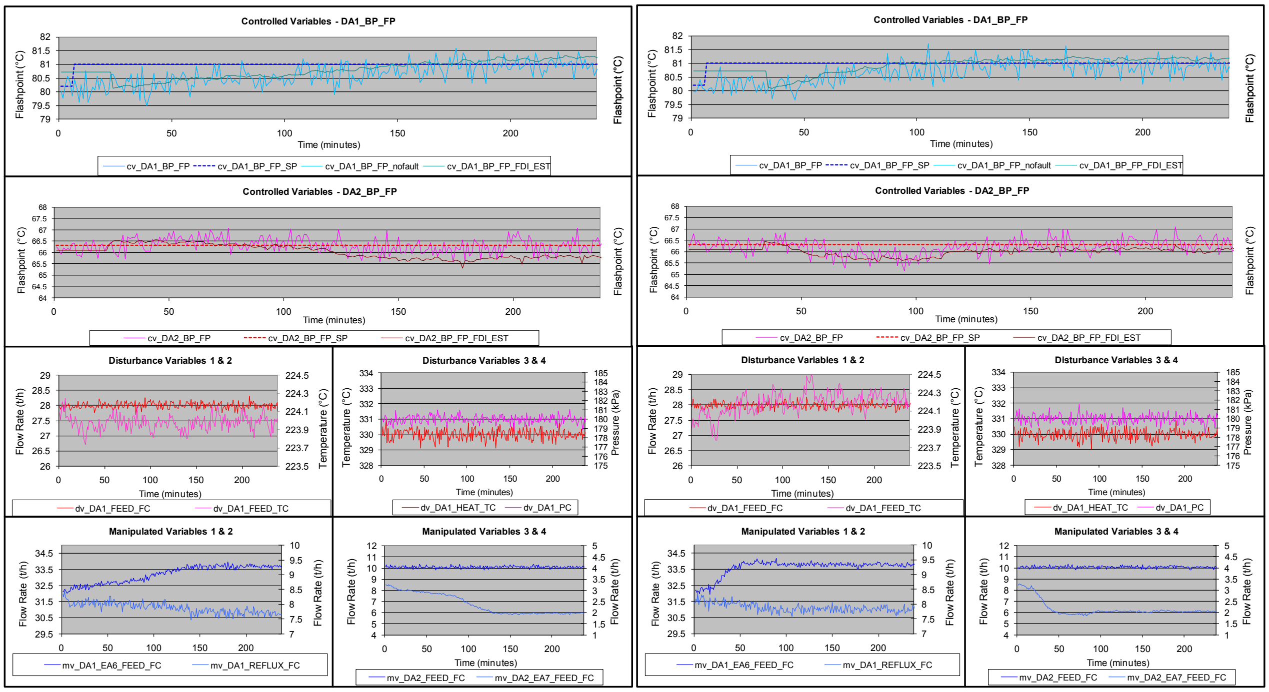

Figure 14. The effects of a stuck valve fault in DA2_FEED_FC while a +1% step change is made to DA1_BP_FP setpoint and without the FTC strategy active (left) and with the FTC strategy active (right).

4.7 Results and discussion

The integrated fault-tolerant MPC was tested with different faults that affect the process; in all the fault cases, the integrated fault-tolerant MPC significantly improved the resistance and response time of the control system to the effect of the faults. With the integrated fault-tolerant MPC, the off-spec production was considerably reduced; the performance of the control system when affected by a fault was improved; and the overall reliability was considerably better than without the integrated FTMPC.

The results of different FTC tests are presented with the reaction times to different fault types in Table 12 for periods when the bottom product flashpoint was off the specification limit with and without the integrated fault-tolerant MPC.

The ISE values were calculated for DA1_BP_FP and DA2_BP_FP in order to compare the results. For a case without any fault, the average ISE for both DA1_BP_FP and DA2_BP_FP was 30. The ISE values for different fault cases, with and without the integrated fault-tolerant MPC, are presented in

Table **13**.

Table 12. Results of the testing of the FTC strategy with different fault types (*compared to a case without a fault).

Tested variable	Fault type	Detection time	Product off spec, without FTC	Product off spec, with FTC
CV Sensor fault	+5% Bias	*3 minutes*	*90 minutes*	*10 minutes*
CV Sensor fault	+5% Drift	*19 minutes*	*90 minutes*	*0 minutes*
DV Sensor fault	-5% Bias	*20 minutes*	*90 minutes*	*25 minutes*
MV Sensor fault	-10% Bias	*16 minutes*	*40 minutes*	*10 minutes*
MV actuator fault	Stuck valve	*3 minutes*	*125 minutes**	*25 minutes**

Table 13. ISE values of the target process with and without FTC and the percentages of improvement with the nominal ISE level of 30.

Tested variable	DA1_BP/DA2_BP ISE, without FTC	DA1_BP/DA2_BP ISE, with FTC	Improvement
CV Sensor fault (+5% bias)	1223 / 114	*27 / 30*	*98 / 74 %*
CV Sensor fault (+5 % drift)	396 / 57	*23 /27*	*94 / 51 %*
DV Sensor fault (-5% bias)	48 / 38	*32 /38*	*43 / 0 %*
MV Sensor fault (-10% bias)	46 / 147	*30 / 66*	*35 / 66 %*
MV actuator fault (stuck valve)	75 / 30	*64 / 30*	*15 / 0 %*

As can be seen from Table 12 and Table 13 the off-spec production was reduced as a result of fast detection and compensation of the faults; the performance of the MPC was also considerably improved with the integrated fault-tolerant MPC. Based on these results, it can be concluded that although the CV faults have longer lasting and more severe effects, the lower level controller faults also have an effect on the overall performance of the control system. Therefore, the usage of the integrated fault-tolerant MPC taking into account faults in DVs and MVs has a definitive effect on the control system performance.

4.8 Economic evaluation of the developed fault-tolerant MPC

Overall, it is estimated that the integrated fault-tolerant MPC has the potential to generate maximum savings of some USD 143,000 during one year in the case of one feed grade alone. If the FTC is used with the other feed grades in addition to the most expensive heavy feed grade used in this study, the savings are even higher, even though the savings with the other grades are not as substantial as with the heavy grade feed. Over 90% of the savings are achieved by more optimal plant operation by reducing the effect of analyser faults through the use of fault accommodation. Less than 10% of the savings are achieved with the active data-based FTC strategy on the DV and MV sensor fault accommodation and controller reconfiguration methods for stuck valve faults. These savings are calculated by using actual plant laboratory and online analyser data, and by measuring the amount of faults in the plant with the following assumptions:

- The price of a bottom product loss in column DA1 is the price difference between the solvent product and the bulk product using the same feedstock type (e.g. diesel or gasoline). The bottom product loss in this case can be estimated to be approximately USD 100 /t.

- The feed level to the unit is 28 t/h; the average bottom product flow rate 17 t/h; the average side product flow rate 9 t/h; and the average overhead distillate flow rate 2 t/h.

- If the product FP goes below the specification limit, it needs to be corrected by preparing an over-quality bottom product for an equivalent time. The quality of the bottom product can be increased by 1°C by increasing the overhead distillate flow by an average of 2 t/h; or alternatively by decreasing the unit feed by 2 t/h on average. In essence, an increase in the overhead distillate flow rate or a decrease in the feed flow rate causes the unit to lose capacity of 2 t/h on average for 1°C of FP. At the same time, the bottom product flow rate also decreases by 2 t/h. We assume 1°C of FP correction is used for all cases.

- The side product flow rate is assumed to be at a maximum, which forces an increase in the overhead flow rate or a decrease in the feed rate in order to correct the off spec batch.

- The over-quality of the final product has the effect that in order to produce an over-quality product, the overhead distillate flow rate has to be increased and the bottom product flow rate reduced, essentially losing capacity of the unit by 2 t/h for 1°C of FP over-quality in the final product.

In general, based on industrial experience of project costs and cost estimates, it could be estimated that an industrial-scale version of the FTMPC without an MPC implementation would cost approximately USD 50,000 – 100,000. Therefore, an integrated FTMPC like this would have a repayment period of four to eight months, thereby making an investment of this magnitude highly profitable in normal economic conditions. Furthermore, if such an integrated fault-tolerant MPC would be implemented in a process without an MPC already in place, the profits would be even higher due to better optimisation of the target process and lower overall costs, since the implementation could be carried out in connection with the installation of an MPC allowing the design of the integrated fault-tolerant MPC.

5 Conclusions

This work presents an active integrated fault-tolerant MPC for an industrial dearomatization process. Based on the results of the simulation study, the proposed FTMPC is able to counter most of the typical faults in the target process. The profitability of the FMPC was evaluated using estimated prices of the end products and by using the process data and frequency of the faults from the actual full-scale dearomatization process located at the Naantali refinery. Based on the economic evaluation of just one feed grade, the integrated fault-tolerant MPC was found to be highly profitable - the annual estimated savings were a maximum of USD 143,000, thereby allowing the integrated fault-tolerant MPC to pay for itself in less than one year.

The integrated fault-tolerant MPC can be estimated to provide considerable savings in off-spec production, energy consumption and, in general, an improvement in the unit's operation due to faster detection and prevention of the effects of the faults. Therefore, the performance and profitability of the actual industrial-scale dearomatization process will also be significantly enhanced if such an FTC strategy is implemented.

Acknowledgments

The authors gratefully acknowledge the support of Neste Oil Oyj particularly for the background information regarding the actual dearomatization process at the Naantali Refinery and Neste Jacobs Oy for the use of the ProsDS simulation software and the models related to the LARPO dearomatization process.

Supporting Information

This information is available free of charge via the Internet at http://pubs.acs.org/

Appendix

A.1 Description of the nonlinear iterative partial least squares-algorithm

The recursive NIPALS algorithm by Wold et al.[20] is presented here to obtain the matrices needed for PLS regression. For two data blocks, X (N by K matrix) and Y (N by M matrix), the NIPALS is carried out iteratively as follows:

1. Select a K-weight vector w, for instance a normalised, non-zero row of X.
2. Calculate the score vector $t=X \cdot w$.
3. Calculate the Y-loading vector $q=Y^{\mathrm{T}} \cdot t$.
4. Calculate the Y-score vector $u=Y \cdot q$.
5. Calculate a new weight vector $w_1=X^{\mathrm{T}} \cdot u$. Scale w_1 to length 1.
6. If $|w-w_1|$ < convergence limit (user-defined), the convergence is obtained, otherwise $w=w_1$ and start at stage 2.

Here N is the number of samples, K is number of input variables and M is number of output variables. Now two score vectors, t (for X) and u (for Y) have been acquired. To acquire the next pair of t and u, several methods are available; however in this context, in the following stages 7-11 by Wold et al.[20], X is adjusted for the score vector and the regression of Y to t is calculated and finally Y is adjusted to the new results.

7. X loading vector p is now calculated with $p = X^T \cdot t/(t^T \cdot t)$
8. Adjust X: $X_{new}=X-t \cdot p^T$
9. Calculate regression of Y to t: $b = (Y^T \cdot t)/(t^T \cdot t)$
10. Adjust Y: $Y_{new} = Y-t \cdot b^T$
11. If more (t,u) pairs are needed, go back to stage 1 by using $X=X_{new}$ and $Y = Y_{new}$

12. If all the needed pairs of *(t,u)* have been acquired, the estimated Y_{pred} can be calculated from $Y_{pred} = T \cdot Q^T = X \cdot W \cdot Q^T = X \cdot R_{PLS}$, where R_{PLS} (K by N matrix) is the regression matrix, T is the scores matrix, W is the weights matrix and Q is the loadings matrix.

Literature Cited

(1) Venkatasubramanian, V.; Rengaswamy, R.; Kavuri, S.N. A review of process fault detection and diagnosis. Part I: Quantitative model-based methods. *Computers & Chemical Engineering* **2003**, *27(3)*, 293–311.

(2) Zhang, Y.M.; Jiang, J. Bibliographical review on reconfigurable fault-tolerant control systems. *Annual Reviews in Control* **2008**, *32(2)*, 229–252.

(3) Campo, P.J.; Morari, M. Robust Model Predictive Control. *In proceedings of 6th American Control Conference* **1987**, Edgar, T.F. (Editor), American Automatic Control Council, Minneapolis, 1021–1026.

(4) Bemporad, A.; Borrelli, F.; Morari, M. Min–max Control of Constrained Uncertain Discrete-Time Linear Systems. *IEEE Transactions on Automatic Control* **2003**, *48(9)*, 1600–1606.

(5) Lazar, M.; Muñoz de la Peña, D.; Heemels, W.P.M.H; Alamo, T. On input-to-state stability of min–max nonlinear model predictive control. *Systems & Control Letters* **2008**, *57(1)*, 39–48.

(6) Huang, R.; Patwardhan, S.C.; Biegler, L.T. Multi-Scenario-Based Robust Nonlinear Model Predictive Control with First Principle Models. *Computer-Aided Chemical Engineering* **2009**, Alves, R., Nascimento C. & Biscaia, E. Jr. (Editors), Elsevier, Amsterdam, 1293–1298.

(7) Pranatyasto, T.N.; Qin, S.J. Sensor validation and process fault diagnosis for FCC units under MPC feedback. *Control Engineering Practice* **2001**, *9(8)*, 877–888.

(8) Prakash, J.; Patwardhan, S.C.; Narasimhan, S.A. Supervisory Approach to Fault-Tolerant Control of Linear Multivariable Systems. *Industrial & Engineering Chemistry Research* **2002**, *41(9)*, 2270–2281.

(9) Mhaskar, P.; Gani, A.; McFall, C.; Christofides, P.D.; Davis, J.F. Fault-tolerant control of nonlinear process systems subject to sensor faults. *AIChE Journal* **2007**, *53(3)*, 654–668.

(10) Koivisto, K.; Kettunen, M.; Sourander, M.; Liikala, T.; Léger, J.-B.; Sauter, D. Fault-tolerant control protects processes and products. *Hydrocarbon processing* **2008**, *87(10)*, 51–61.

(11) Deshpande, A.P.; Patwardhan, S.C.; Narasimhan, S.S. Intelligent state estimation for fault tolerant nonlinear predictive control. *Journal of Process Control* **2009**, *19(2)*, 187–204.

(12) Kettunen, M. Data-Based Fault-Tolerant Model Predictive Controller: An Application to a Complex Dearomatization Process, *Doctoral thesis* **2010**, Aalto University of Science and Technology, Espoo. Available online: *http://lib.tkk.fi/Diss/2010/isbn9789526032016/*

(13) Mahmoud, M.M.; Jiang, J.; Zhang, Y.M. Active fault tolerant control systems: Stochastic analysis and synthesis. *Lecture notes in control and information sciences (Vol. 287)* **2003**, Springer-Verlag, Berlin.

(14) Bao, J.; Zhang, W.Z.; Lee, P.L. Decentralized fault-tolerant control system design for unstable processes. *Chemical Engineering Science* **2003**, *58(22)*, 5045–5054.

(15) Dunia, R.; Qin, S.J.; Edgar, T.F.; McAvoy, T. Identification of Faulty Sensors Using Principal Component Analysis. *AIChE Journal* **1996**, *42(10)*, 2797–2812

(16) Vermasvuori, M. Methodology for utilising prior knowledge in constructing data-based process monitoring systems with an application to dearomatization process. *Doctoral dissertation* **2008**, Helsinki University of Technology, Espoo.

(17) Mhaskar, P.; Gani, A.; El-Farra, N.H.; McFall, C.; Christofides P.D.; Davis, J. F. Integrated Fault Detection and Fault-Tolerant Control of Process Systems. *AIChE Journal* **2006**, *52(6)*, 2129-2148.

(18) Mhaskar, P.; Gani, A.; Christofides, P.D. Fault-Tolerant Control of Nonlinear Processes: Performance-Based Reconfiguration and Robustness. *International Journal of Robust and Nonlinear Control* **2006**, *16*, 91-111.

(19) Mhaskar, P.; McFall, C.; Gani, A.; Christofides, P.D.; Davis, J.F. Isolation and Handling of Actuator Faults in Nonlinear Systems. *Automatica* **2008**, *44*, 53-62.

(20) Wold, S.; Martens, H.; Wold, H. The multivariate calibration problem in chemistry solved by the PLS method. *In: Proceedings of Conference Matrix Pencils, Ruhe A. & Kågstørm, B. (Editors), Lecture Notes in Mathematics* **1983**, Springer-Verlag, Heidelberg, 286-293.

(21) Buffington, J.M.; Enns, D.F. Lyapunov Stability Analysis of Daisy Chain Control Allocation. *Journal of Guidance, Control and Dynamics* **1996**, *19(6)*, 1226–1230.

(22) Maciejowski, J.M. The Implicit Daisy-Chaining Property of Constrained Predictive Control. *Applied mathematics and Computer Science* **1998**, *8(4)*, 101–117.

(23) Alwi, H.; Edwards, C. Fault tolerant control using sliding modes with on-line control allocation. *Automatica* **2008**, *44(7)*, 1859–1866.

(24) Maciejowski, J.M. Predictive Control with Constraints. **2002,** Prentice Hall, London.

(25) Vermasvuori, M.; Vatanski, N.; Jämsä-Jounela, S-L. Data-based fault detection of the online analysers in a dearomatisation process. *In: Proceedings of 1st NeCST workshop on Networked Control Systems & Fault Tolerant Control* **2005**, 219–224.

(26) Liikala, T. The use of fault detection in model predictive control of a refinery process unit. *Master's Thesis* **2005**, Espoo: Helsinki University of Technology.